

Synthesis and Characterization of Novel Zirconium Oxide-Crystalline Cerium(IV)Hydrogen Phosphate/ Polybenzimidazole, Polyaniline, Polyindole, Polycarbazole, Nanocomposites

S. K. Shakshooki (Corresponding Author)

Department of Chemistry Faculty of Science, University of Tripoli, Tripoli, Libya.

Email: shakshooki2002@yahoo.com

A. A. Jangher

Department of Chemistry Faculty of Science, University of Tripoli, Tripoli, Libya.

F. A. Elakari

Department of Chemistry Faculty of Science, University of Tripoli, Tripoli, Libya.

M.O. Darwish

Department of Chemistry Faculty of Science, University of Tripoli, Tripoli, Libya.

S. M. El-Hamroni

Department of Chemistry Faculty of Science, University of Tripoli, Tripoli, Libya.

Article History

Received: 20 October, 2023

Revised: 24 December, 2023


Accepted: 19 January, 2024

Published: 25 January, 2024

Copyright © 2024 ARPG & Author

This work is licensed under the Creative Commons Attribution International

Attribution International

 CC BY: Creative Commons Attribution License

4.0

Abstract

Crystalline cerium (iv) hydrogen phosphate $Ce(HPO_4)_2 \cdot 1.33H_2O$ (CeP), and nano particles zirconium oxide ($nZrO_2$), of average size 19.3nm, were prepared and characterized by chemical, XRD, FT-IR and TGA analysis. Mixing slurry aqueous solution of $nZrO_2$ and CeP in 25:75 wt/wt% mixing ratios, respectively, lead to formation of novel zirconium oxide-crystalline cerium phosphate nanocomposite, $[ZrO_2]_{0.25}[Ce(HPO_4)_2]_{0.75} \cdot 1.33H_2O$ ($nZrO_2$ -CeP). Novel $[nZrO_2]_{0.25}[CeP]_{0.75}$ polybenzimidazole-, polyaniline-, polyindole-, and polycarbazole nanocomposites were prepared via in-situ chemical oxidation of their parent monomers. A possible explanation is part of CeP, in inorganic composite ($nZrO_2$ -CeP) was attacked by the parent monomers converted to cerium(III) orthophosphate ($CePO_4$). The resultant nanocomposites were characterized by elemental (C,H,N) analysis, FT-IR, and scanning electron microscopy (SEM). From elemental (C,H,N) analysis, the amount of % in wt. of organic materials present in ($nZrO_2$ -CeP) nanocomposites found to be, for [polybenzimidazole (12.56%), polyaniline (16.50%), polyindole (11.74%), and polycarbazole (13.99%)]. Electrical conductivity for resultant conducting polymers were investigated using DMSO solvent found to be in the range of semiconductors.

Keywords: Crystalline cerium(iv)hydrogen phosphate; Nano zirconium oxide; Polybenzimidazole; Polyaniline; Polyindole; Polycarbazole; Nanocomposites.

1. Introduction

Electronically conducting polymers exhibit wide range of electrical conductivity from semiconductors to metallic region by way of doping. Have been the subject of great interest in recent years [1, 2]. Called as synthetic metals because of their enormous interesting properties like high electric conductivity, environmental and chemical stability, low cost, easy prepared by chemical oxidative polymerization and electrochemical methods and fast reversible doping and de-doping [3-6]. Out of these two methods, chemical polymerization is preferred [2, 6]. Conducting polymers are a novel class of synthetic metals that combine the chemical, electrochemical and mechanical properties of polymers with the electronic properties of metals and semiconductor. Have potential applications in various fields such as rechargeable batteries, electrochromic display device separation membranes, sensors and anticorrosive for metals etc. [1-11].

Heterocyclic conducting polymers, containing nitrogen atoms like, polypyrrole, polyindole and polyaniline, also their substituted derivatives have received increasing attention in various fields, such as electronics, sensors, and others [12-14]. Their electrical and electrochemical properties show great promise for commercial applications makes their use as metal replacement materials [12-17].

Transition metal oxides composed of oxygen atoms bound to transition metals. They are commonly utilized for their catalytic activity and Semi-conductive properties. They also frequently used as pigments in paints and plastics, most notably titanium dioxide. Transition metal oxides have a wide variety of surface structures which affect the surface energy of these compounds and influence their chemical properties [18-20].

Most transition metals have more than one oxidation state. Wide varieties of nanostructures for metal oxides are reported (e.g., TiO_2 , ZrO_2 , SnO_2 , NiO , CeO_2 , Nb_2O_5 , Fe_2O_3 , Co_3O_4), have been heavily investigated [19, 20].

Crystalline cerium phosphates have been studied for a long time as ion exchangers, their structures remains unknown until recently [21]. The reason is that, the composition, the structure and the degree of crystallinity of their precipitates results from reaction of solutions containing a Ce(IV) salt which is mixed with a solution of phosphoric

acid of $[(\text{PO}_4)/\text{Ce}(\text{IV}) \text{ ratio}]$, strongly depend on the experimental conditions such as rate and order of mixing of the solutions, stirring, temperature and digestion time, this also implemented on fibrous cerium phosphate [22-26].

2. Materials and Methods

2.1. Chemicals

$\text{Ce}(\text{SO}_4)_2 \cdot 4\text{H}_2\text{O}$, $\text{ZrOCl}_2 \cdot 8\text{H}_2\text{O}$, H_3PO_4 (85%), dimethyl sulfoxide (DMSO) of BDH, aniline (99.5%) of Mindex UK, indole, carbazole of Reild de-Haiden, crystalline benzimidazole was synthesized and characterized by CHN analysis FT-IR & Mpt., ethanol 95% of Sigma. Other reagents used were of analytical grade.

2.2. Instruments Used for Analysis

X-ray powder diffractometer. Siemens D-500, using Ni-filtered $\text{Cu K}\alpha$ ($\lambda = 1.54056 \text{ \AA}$) XRD with $\text{CuK}\alpha$ radiation at 1.540 \AA by using Philips PW1710, Scanning electron microscopy (SEM) Jeol SMJ Sm 5610 LV, Fourier Transform infrared spectrometer FT-IR, FT-IR-6100 and Shimadzu FT-IR Spectrometer in the range $200\text{--}4000 \text{ cm}^{-1}$, Carbon Hydrogen Nitrogen (CHN) automatic analyzer Varian EL III-Elemental, Germany, pH Meter WGW 521, Ultraviolet-Visible (UV-vis) Perkin Elmer Life and Analytical sciences, 710, Bridgeport Shelton, USA and Conductivity meter 4510 from JENWAY.

2.3. Preparation of Crystalline Cerium Phosphate

To 25g $\text{CeSO}_4 \cdot 4\text{H}_2\text{O}$, 100 ml H_3PO_4 (10 M) were added, subjected to reflux at $80 \text{ }^\circ\text{C}$ for 100h. The product subject to washing up to $\text{pH} \sim 3.5$, filtered and air dried. The color of the product was yellow.

2.4. Preparation of Nano Zirconium Oxide

ZrO_2 nanostructure was prepared by sol-gel technique. To 100 ml of 0.2 M Zirconyl oxychloride octahydrate, ($\text{ZrOCl}_2 \cdot 8\text{H}_2\text{O}$) in beaker, 250 ml of 2.0 M ammonium hydroxide (NH_4OH) were added dropwise with stirring at room temperature ($23 \text{ }^\circ\text{C}$). After complete addition the stirring was continued for 2 h., (Mother liquor mixture $\text{pH} = 9$).. The resultant white gel was filtered on Buchner Funnel, washed with double distilled water up to $\text{pH} = 3$., dried in oven at $110 \text{ }^\circ\text{C}$ for 2 h. then calcined at $600 \text{ }^\circ\text{C}$ for about 3 h, zirconium dioxide nanoparticle was obtained.

2.5. Preparation of Nano Zirconium Oxide-Crystalline Cerium Phosphate Nano Composite

0.25 g of nZrO_2 was mixed with 0.75 g of crystalline cerium phosphate, $\text{Ce}(\text{HPO}_4)_2 \cdot 1.33\text{H}_2\text{O}$, solid-solid mixing, then was dispersed in 10 ml ethanol with stirring for 30 minutes at room temperature. The resultant product was filtered, washed with ethanol and left to dry in air.

2.6. Polymerization of Benzimidazole, Aniline, Indole and Carbazole by $[\text{ZrO}_2]_{0.25}[\text{CeP}]_{0.75}$ Nano Composite

2.6.1. Polymerization of Benzimidazole by $[\text{ZrO}_2]_{0.25}[\text{CeP}]_{0.75}$ Nano Composite

$[\text{ZrO}_2]_{0.25}[\text{CeP}]_{0.75}$ /polybenzimidazole nanocomposite was prepared by direct contact of 0.25g $[\text{ZrO}_2]_{0.25}[\text{CeP}]_{0.75}$ composite with 13 ml 4% benzimidazole in ethanol, at room temperature with stirring for 48h. The resultant product was filtered, washed with ethanol and left to dry in air. The color of the product was yellowish..

2.6.2. Polymerization of Aniline by $[\text{ZrO}_2]_{0.25}[\text{CeP}]_{0.75}$ Nanocomposite

$[\text{ZrO}_2]_{0.25}[\text{CeP}]_{0.75}$ /polyaniline nanocomposite was prepared by direct contact of 0.25g of $[\text{ZrO}_2]_{0.25}[\text{CeP}]_{0.75}$ composite with 10 ml 4% aniline in ethanol, at room temperature with stirring for 48 h.. The resultant product was filtered, washed with ethanol and left to dry in air. The color of the product was green.

2.6.3. Polymerization of Indole by $[\text{ZrO}_2]_{0.25}[\text{CeP}]_{0.75}$ Nanocomposite

$[\text{ZrO}_2]_{0.25}[\text{CeP}]_{0.75}$ /polyindole nanocomposite was prepared by direct contact of 0.25g of $[\text{ZrO}_2]_{0.25}[\text{CeP}]_{0.75}$ composite with 18ml 4% indole in ethanol, at room temperature with stirring for 48h. The resultant product was filtered, washed with ethanol and left to dry in air. The color of the product was brown.

2.6.4. Polymerization of Carbazole by $[\text{ZrO}_2]_{0.25}[\text{CeP}]_{0.75}$ Nanocomposite

$[\text{ZrO}_2]_{0.25}[\text{CeP}]_{0.75}$ /polycarbazole nanocomposite was prepared by direct contact of 0.25 g of $[\text{ZrO}_2]_{0.25}[\text{CeP}]_{0.75}$ composite with 13 ml 4% carbazole in THF, at room temperature with stirring for 48 h.. The resultant product was filtered, washed with ethanol and left to dry in air. The color of the product was light-green.

2.6.5. Electrical Conductivity Measurements

Conductivity measurements were carried out at ($25 \text{ }^\circ\text{C}$) (using 4510 conductivity meter, JENWAY) as follows:

0.1 g of each of the resultant $[\text{ZrO}_2]_{0.25}[\text{CeP}]_{0.75}$ /polymer nanocomposite was dissolved in 10 ml DMSO. After calibration the measurement of samples is carried out by immersing the cell in the samples, allowing the readout to stabilize, and recording the result. The cell were rinsed with deionized water between each sampling to avoid contamination, shaken to remove internal droplets, and the outside wiped by DMSO prior immersion in the next

sample. On completion of sample measurement the cell were thoroughly rinsed with deionized water. In similar way conductivity measurements were carried out for the rest of selected samples.

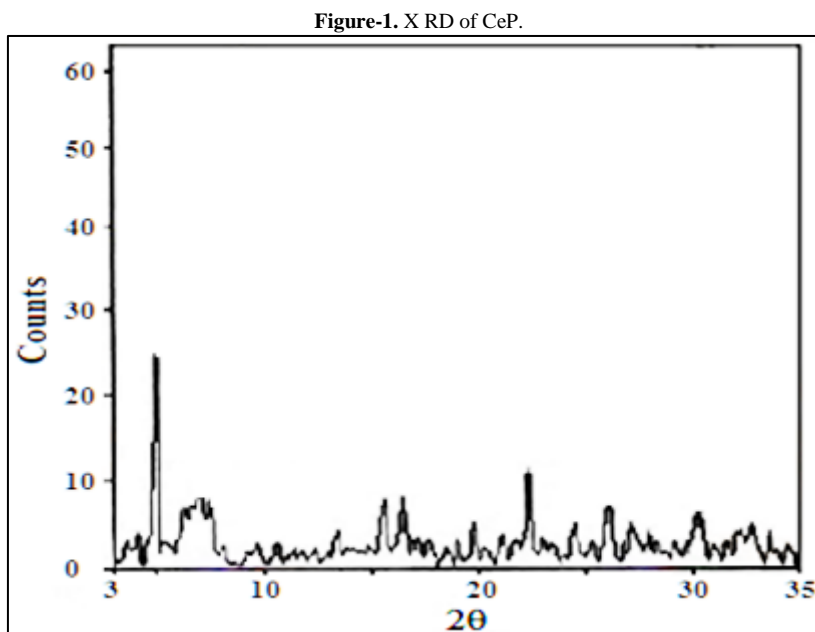
3. Results and Discussion

3.1. Crystalline Cerium Phosphate, $\text{Ce}(\text{HPO}_4)_2 \cdot 1.33\text{H}_2\text{O}$

Crystalline cerium phosphate, $\text{Ce}(\text{HPO}_4)_2 \cdot 1.33\text{H}_2\text{O}$ (CeP), was prepared and characterized by chemical, XRD, TGA and FT-IR spectroscopy.

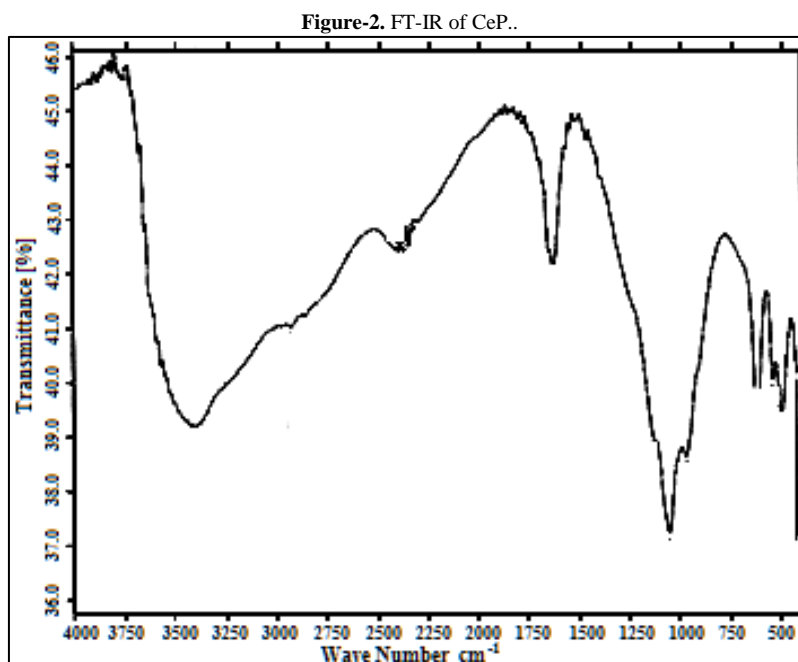
3.1. XRD of CeP

X-ray diffraction pattern of crystalline cerium phosphate is shown in [figure 1](#) Found to be crystalline, with interlayer distance equal to 16.05Å.



3.1.2. FT-IR of CeP

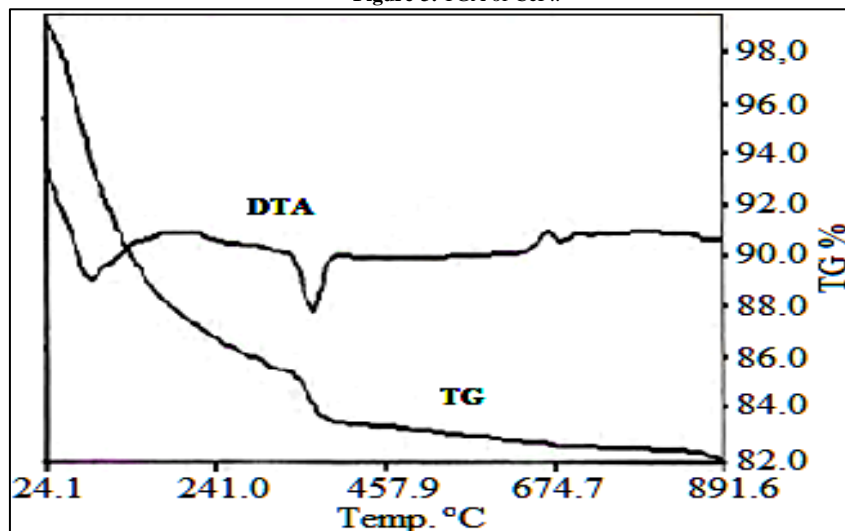
FT-IR spectrum of crystalline cerium phosphate is given in [Figure 2](#). It consist of broad band centered at $\sim 3377\text{cm}^{-1}$ attributed to OH groups symmetric stretching of H_2O . Small sharp band at 1656cm^{-1} is due to H-O-H bending, sharp broad band centered at 1055cm^{-1} is related to the phosphate groups vibration.



3.1.3. TGA of CeP

Thermal analysis of $\text{Ce}(\text{HPO}_4)_2 \cdot 1.33\text{H}_2\text{O}$ is shown in [Figure 3](#) was carried out at temperature range $\sim 25\text{-}90\text{ }^\circ\text{C}$ in air atmosphere. The heating rate was $10\text{ }^\circ\text{C}/\text{min}$. the water of hydration loss occurs in the temperature range $70\text{-}250\text{ }^\circ\text{C}$. Above that POH groups condensation occurs. The final product was $\text{CeO}_2 \cdot \text{P}_2\text{O}_5$.

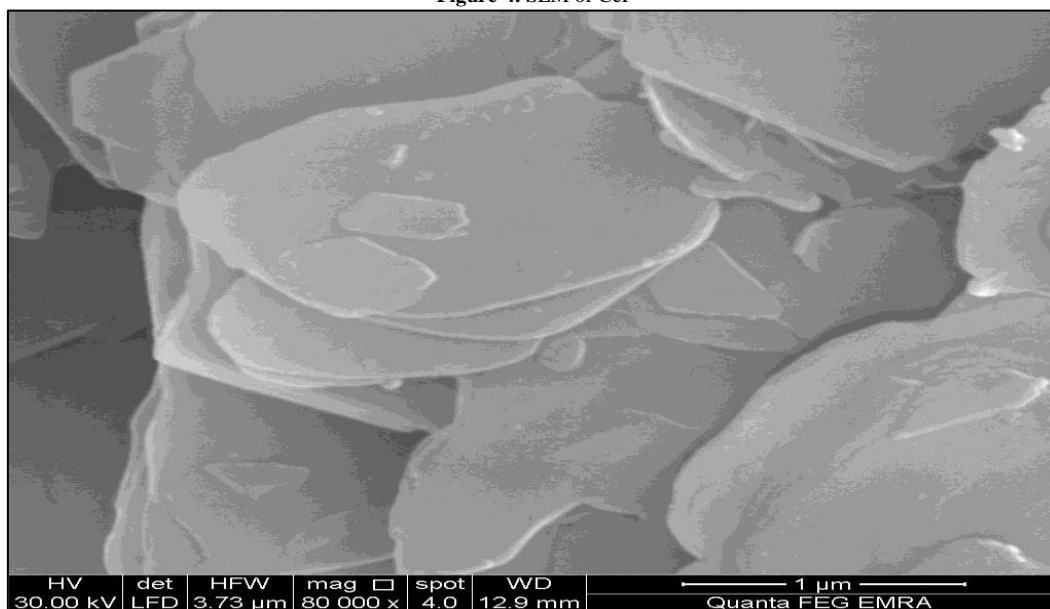
Figure-3. TGA of CeP..



3.1.4 SEM of CeP

SEM morphology image of crystalline cerium phosphate is shown in Figure 4. The photograph shows its in form, mainly, of compact crystallites.

Figure-4. SEM of CeP



3.2. Nano Zirconium Oxide

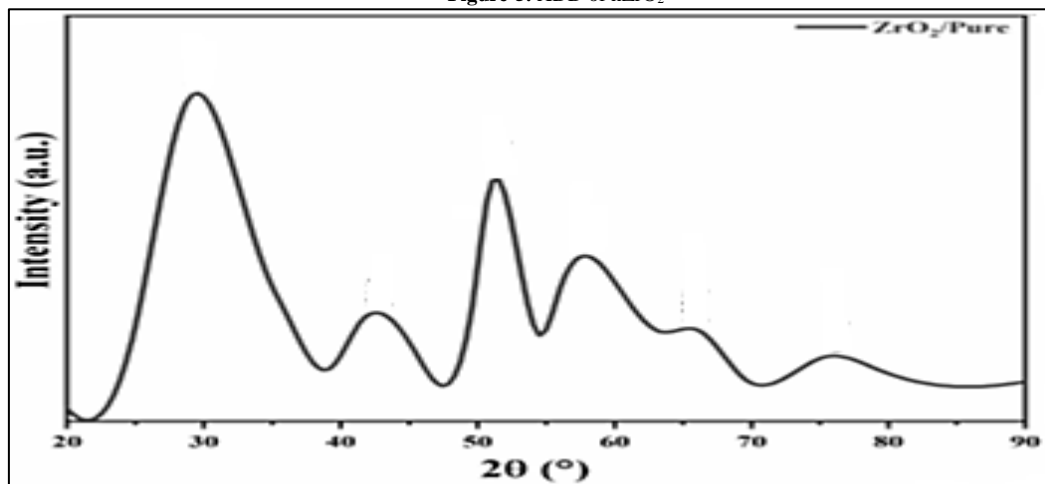
Nano particles zirconium oxide ($n\text{ZrO}_2$), of average size 19.3 nm, were prepared and characterized by chemical, XRD, and FT-IR, found to be similar trend to that already reported [27].

3.2.1. XRD of ZrO_2 Nanoparticle

X-ray diffraction pattern of crystalline $n\text{ZrO}_2$ is shown in Figure 5. Its average diameter D found to be 19.3 nm, which was calculated from the full width at half maximum of the peak using Scherer's equation [28].

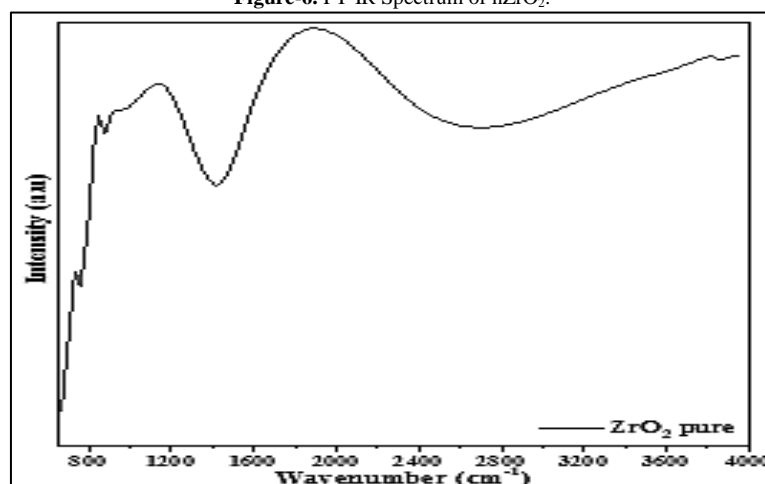
$$D = \frac{0.9\lambda}{B_{2\theta}\cos\theta_{\max}}$$

Where D is the average crystal size in nm, λ is the characteristic wave length of x-ray used ($\lambda=1.54056 \text{ \AA}$), θ is the diffraction angle, and the $B_{2\theta}$ is the angular width in the radius at intensity equal to half of the maximum peak intensity.

Figure-5. XDD of nZrO₂

3.2.2. FT-IR Spectrum of nZrO₂

FT-IR spectrum of nZrO₂ nanoparticle is shown in Figure 6. The broad band centered at 2800 cm⁻¹ and that at 1500 cm⁻¹ correlate with the -OH stretching of adsorbed water [27].

Figure-6. FT-IR Spectrum of nZrO₂.

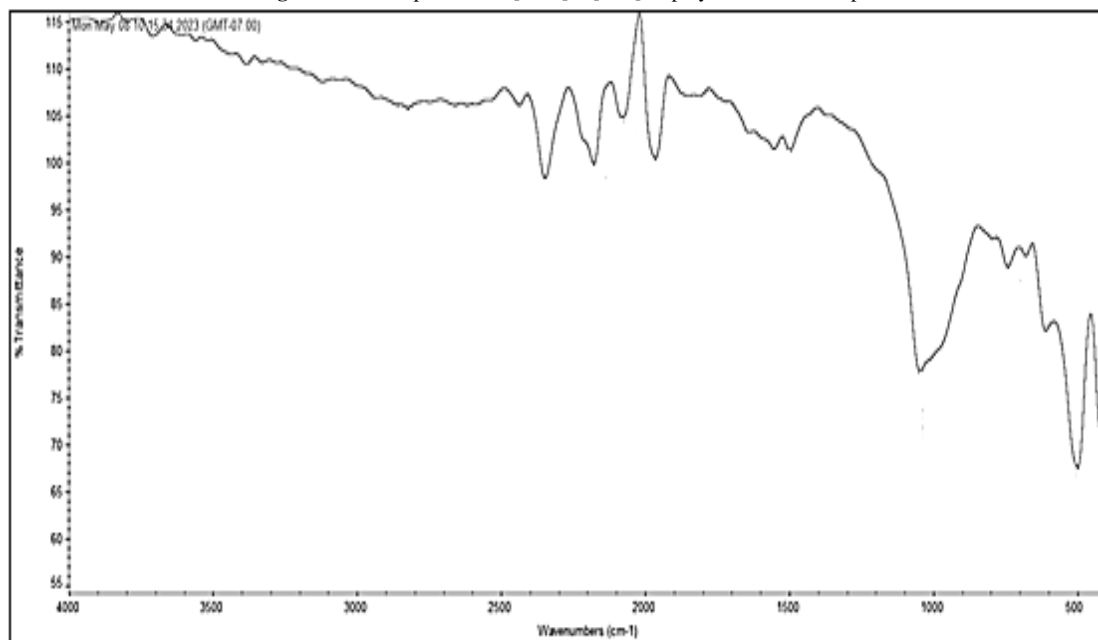
3.3. Elemental (C,H,N) Analysis

Elemental (C,H,N) analysis were carried out. The amount of % in wt. of organic materials present in (nZrO₂-CeP) nanocomposites were for polybenzimidazole (12.56%), for polyaniline (16.50%), for polyindole (11.74%), and for polycarbazole (13.99%).

3.4. FT-IR of [ZrO₂]_{0.25}[CeP]_{0.75}/ Polyaniline, Polybenzimidazole, Polyindole and Polycarbazole Nanocomposites

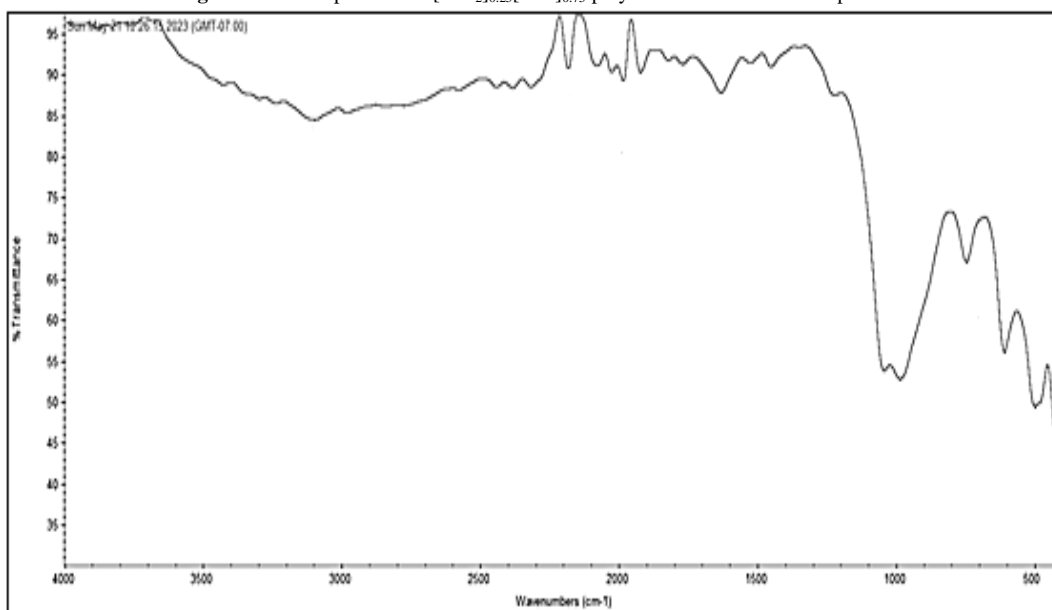
3.4.1. FT-IR of [ZrO₂]_{0.25}[CeP]_{0.75}/Polyaniline Nanocomposite

Figure 7, shows FT-IR spectrum [ZrO₂]_{0.25}[CeP]_{0.75}/polyaniline consists of broad band in the range 3650-2700 cm⁻¹ centered 3094 cm⁻¹ is due to OH groups symmetric stretching of H₂O super imposed with the N-H stretching of aromatic amines, bands at range 2500-1982 cm⁻¹ corresponds to C-H bonds. Band around ~1629 cm⁻¹ is related to H-O-H bending. Other bands in the range 1919-1200 cm⁻¹ correspond to the non-symmetric C₆ ring stretching modes and to C-C bonds C-H (aromatic) stretching, C=C stretching and C-N stretching of the resultant nanocomposite. Broad band in the range 1100-800 cm⁻¹ centered at 1042 cm⁻¹ corresponds to phosphate groups (PO₄) vibration,. Band at 743 cm⁻¹ is relate to CH stretching, band in the range 650-420 cm⁻¹ is correspond to MO bond.

Figure-7. FT-IR spectrum of $[\text{ZrO}_2]_{0.25}[\text{CeP}]_{0.75}$ /polyaniline nanocomposite.

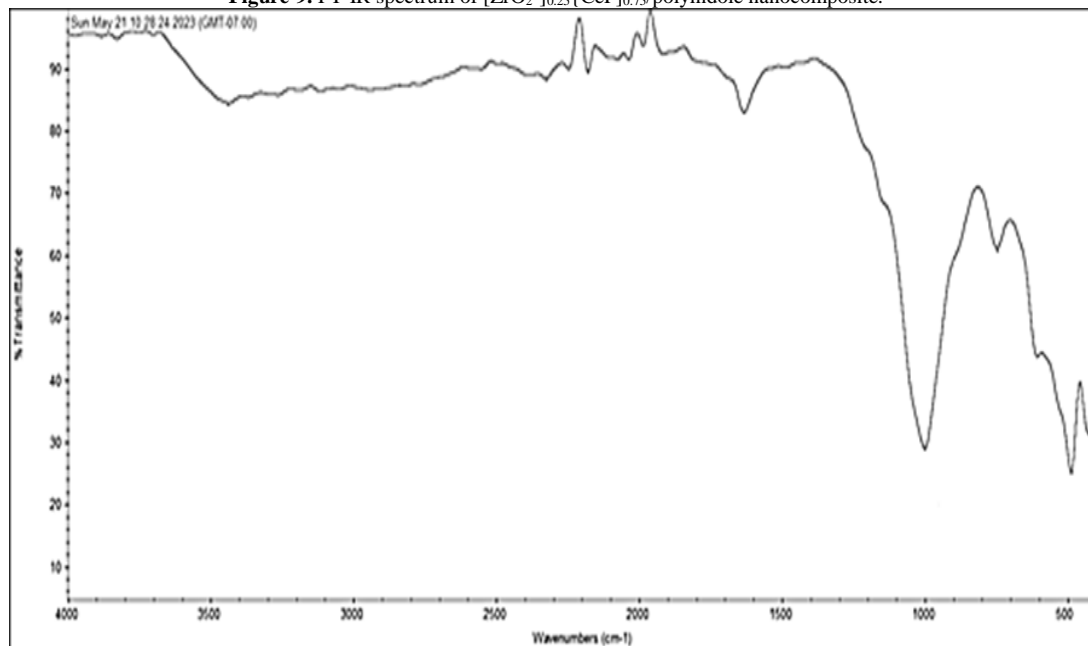
3.4.2. FT-IR Spectrum of $[\text{ZrO}_2]_{0.25}[\text{CeP}]_{0.75}$ /Polybenzimidazole Nano-Composite

Figure 8, shows FT-IR spectrum $[\text{ZrO}_2]_{0.25}[\text{CeP}]_{0.75}$ /polybenzimidazole. consists of broad band in the range $3500\text{--}2700\text{ cm}^{-1}$ centered 3094 cm^{-1} is due to OH groups symmetric stretching of H_2O super imposed with the N–H stretching of aromatic amines ,bands at range $2450\text{--}2000\text{ cm}^{-1}$ corresponds to C-H bonds. Band around $\sim 1629\text{ cm}^{-1}$ is related to H-O-H bending. Other bands in the range $1919\text{--}1200\text{ cm}^{-1}$ correspond to the non-symmetric C_6 ring stretching modes and to C-C bonds C-H (aromatic) stretching, C=C stretching and C-N stretching of the resultant nanocomposite. Broad band in the range $1100\text{--}800\text{ cm}^{-1}$ centered at 1000 cm^{-1} corresponds to phosphate groups (PO_4) vibration,. Band at 743 cm^{-1} is relate to CH stretching, band in the range $6064\text{--}96\text{ cm}^{-1}$ is correspond to MO.

Figure-8. FT-IR spectrum of $[\text{ZrO}_2]_{0.25}[\text{CeP}]_{0.75}$ /polybenzimidazole nanocomposite.

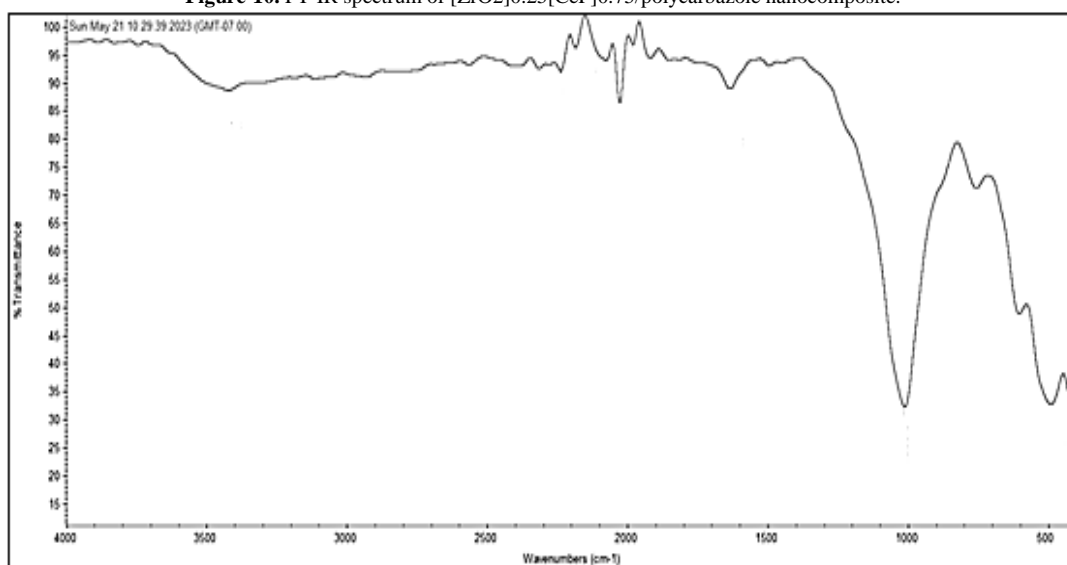
3.4.3. FT-IR Spectrum of $[\text{ZrO}_2]_{0.25}[\text{CeP}]_{0.75}$ /Polyindole Nanocomposite

Figure 9, shows FT-IR spectrum $[\text{ZrO}_2]_{0.25}[\text{CeP}]_{0.75}$ /polyindole consists of broad band in the range $3650\text{--}3000\text{ cm}^{-1}$ centered 3436 cm^{-1} is due to OH groups symmetric stretching of H_2O super imposed with the N–H stretching of aromatic amines ,bands at range $2326\text{--}2100\text{ cm}^{-1}$ corresponds to C-H bonds. Band around $\sim 1631\text{ cm}^{-1}$ is related to H-O-H bending. Other bands in the range $1900\text{--}1200\text{ cm}^{-1}$ correspond to the non-symmetric C_6 ring stretching modes and to C-C bonds C-H (aromatic) stretching, C=C stretching and C-N stretching of the resultant nanocomposite. Broad band in the range $1100\text{--}850\text{ cm}^{-1}$ centered at 967 cm^{-1} corresponds to phosphate groups (PO_4) vibration,. Band at 744 cm^{-1} is relate to CH stretching, band in the range $600\text{--}495\text{ cm}^{-1}$ is correspond to MO bond.

Figure-9. FT-IR spectrum of $[\text{ZrO}_2]_{0.25}[\text{CeP}]_{0.75}$ /polyindole nanocomposite.

3.4.4. FT-IR Spectrum of $[\text{ZrO}_2]_{0.25}[\text{CeP}]_{0.75}$ /Polycarbazole Nanocomposite

Figure 10, shows FT-IR spectrum / polycarbazole consists of broad band in the range 3600-3200 cm^{-1} centered 3421 cm^{-1} is due to OH groups symmetric stretching of H_2O super imposed with the N-H stretching of aromatic amines, bands at range 2236-1950 cm^{-1} corresponds to C-H bonds. Band around $\sim 1632 \text{ cm}^{-1}$ is related to H-O-H bending. Other bands in the range 1900-1200 cm^{-1} correspond to the non-symmetric C_6 ring stretching modes and to C-C bonds C-H (aromatic) stretching, C=C stretching and C-N stretching of the resultant nanocomposite. Broad band in the range 1180-850 cm^{-1} centered at 1009 cm^{-1} corresponds to phosphate groups (PO_4) vibration,. Band at 750 cm^{-1} is relate to CH stretching, band in the range 620-450 cm^{-1} is correspond to MO bond.

Figure-10. FT-IR spectrum of $[\text{ZrO}_2]_{0.25}[\text{CeP}]_{0.75}$ /polycarbazole nanocomposite.

3.5. SEM of $[\text{ZrO}_2]_{0.25}[\text{CeP}]_{0.75}$ /Polybenzimidazole, Polyaniline, Polyindole and Polycarbazole Nanocomposites.

SEM morphology images of $[\text{ZrO}_2]_{0.25}[\text{CeP}]_{0.75}$ / polyaniline, polybenzimidazole, polyindole and polycarbazole nanocomposites are shown in Figures 11, 12, 13, 14, respectively, reveal a uniform distribution of the resultant polymers on the inorganic matrix.

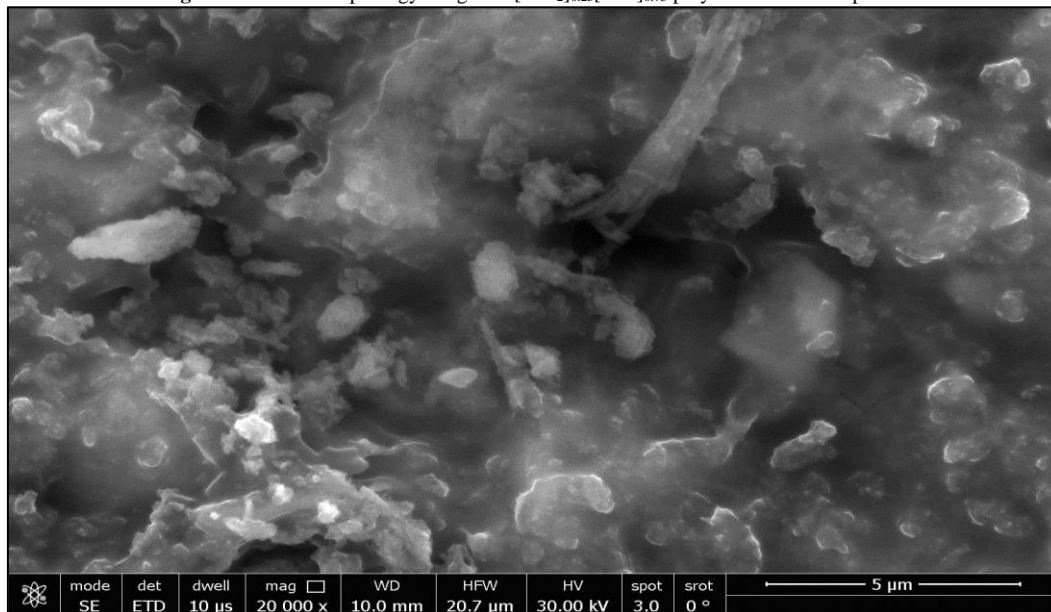
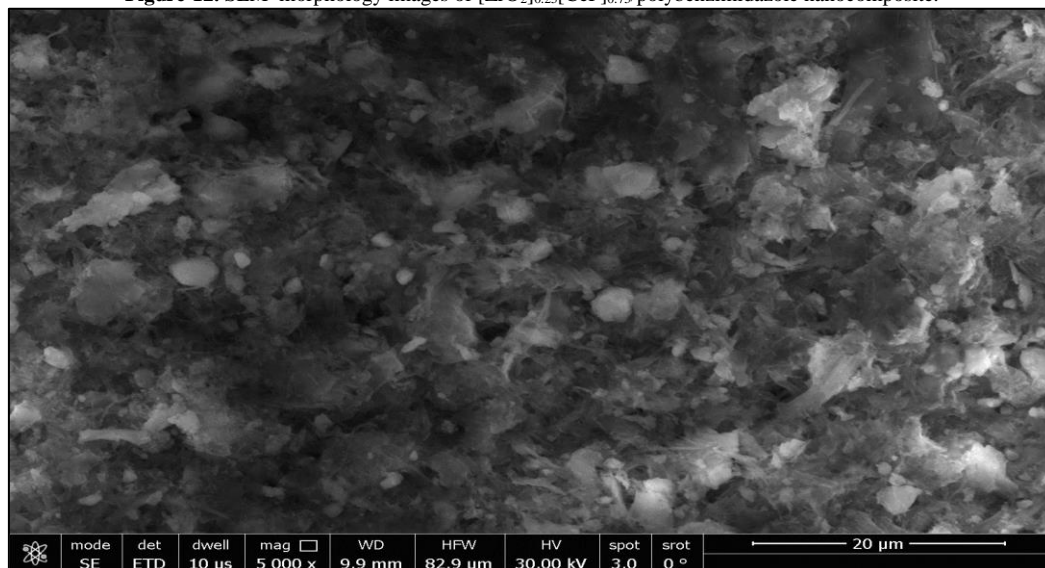
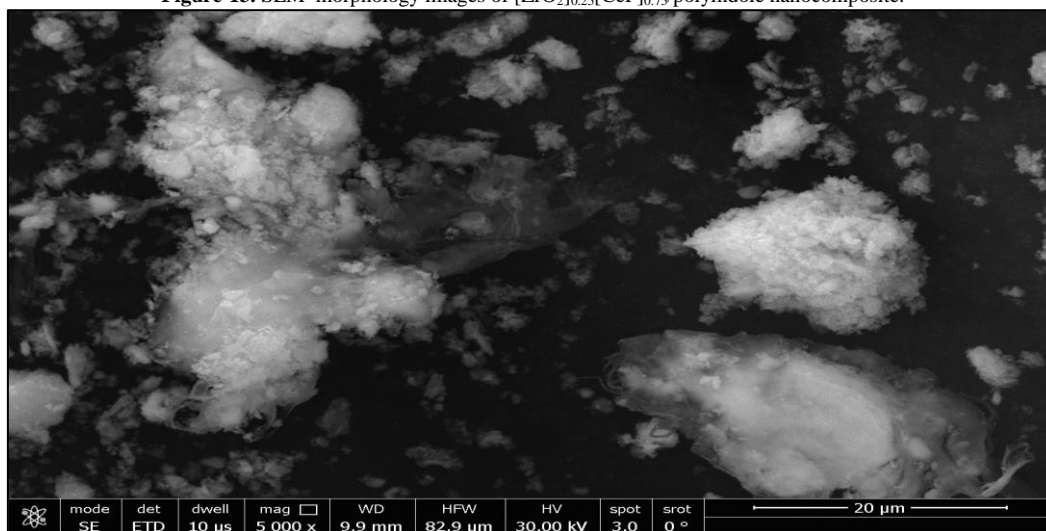
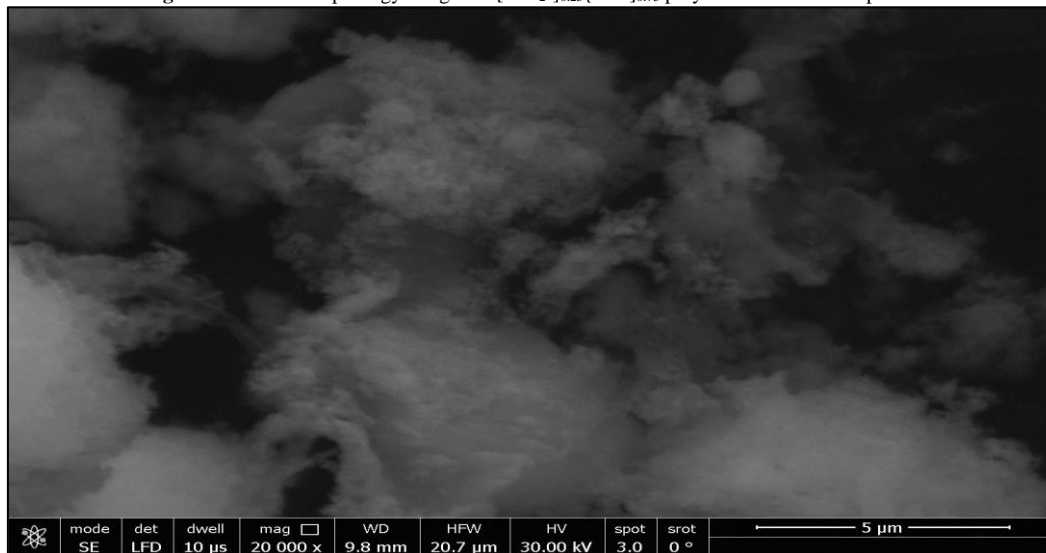
Figure-11. SEM morphology images of $[\text{ZrO}_2]_{0.25}[\text{CeP}]_{0.75}$ /polyaniline nanocomposite.**Figure-12.** SEM morphology images of $[\text{ZrO}_2]_{0.25}[\text{CeP}]_{0.75}$ /polybenzimidazole nanocomposite.**Figure-13.** SEM morphology images of $[\text{ZrO}_2]_{0.25}[\text{CeP}]_{0.75}$ /polyindole nanocomposite.

Figure-14. SEM morphology images of $[\text{ZrO}_2]_{0.25}[\text{CeP}]_{0.75}$ polycarbazole nanocomposite.

3.6. Electrical Conductivity

Electrical conductivity is defined as the ratio of the current density to the electric field strength and can be expressed as:

$\sigma = J/E$, where σ = electrical conductivity ($1/\text{ohms m}$, $1/\Omega \text{ m}$, siemens/m, S/m, mho/m), J = current density (amps/m^2), E = electric field strength (volts/m).

Table 1 represents the conductivity of extracted resultant conducting polymers, polybenzimidazole, polyaniline, polyindole and polycarbazole from their nanocomposites.

Table-1. Electrical conductivity of extracted polybenzimidazole, polyaniline, polyindole and polycarbazole from their tetravalent metal tellurates composites

No.	Samples	Electrical conductivity ($\Omega \text{ Cm}^{-1}$)
	$[\text{ZrO}_2]_{0.25}[\text{CeP}]_{0.75}/\text{polybenzimidazole}$	1.00×10^{-5}
	$[\text{ZrO}_2]_{0.25}[\text{CeP}]_{0.75}/\text{polyaniline}$	1.00×10^{-5}
	$[\text{ZrO}_2]_{0.25}[\text{CeP}]_{0.75}/\text{polyindole}$	1.00×10^{-4}
	$[\text{ZrO}_2]_{0.25}[\text{CeP}]_{0.75}/\text{polycarbazole}$	1.0×10^{-4}

5. Conclusion

Crystalline cerium (iv) hydrogen phosphate $\text{Ce}(\text{HPO}_4)_2 \cdot 1.33\text{H}_2\text{O}$ (CeP), and nano particles zirconium oxide ($n\text{ZrO}_2$) of average size 19.3nm, were prepared and characterized by chemical, XRD, FT-IR and TGA analysis. Novel zirconium oxide-crystalline cerium phosphate nanocomposite, $[\text{ZrO}_2]_{0.25}[\text{Ce}(\text{HPO}_4)_2]_{0.75}$. was prepared and characterized.

The direct oxidation polymerization method of conjugated organic heterocyclic monomers and aniline is the most communal method used for synthesis of their CPs. However, self-support polymerization method is new approach for the synthesis of conducting polymers composites, that was implemented for the synthesis of the resultant novel polybenzimidazole, polyaniline-, polyindole-, and polycarbazole nano composites from their parent monomers using novel $[\text{ZrO}_2]_{0.25}[\text{CeP}]_{0.75}$ nanocomposite that were characterized by CHN, FT-IR and SEM analysis. The color of the resultant conducting polymers nanocomposites support the formation of the composites. Their electrical conductivity found to be in range of semiconductors.

Acknowledgements

To Department of Chemistry, Faculty of Science, University of Tripoli for providing facilities for this research.

References

- [1] Skotheim, T. and Reynolds, J. R., 1997. *Eds., handbook of conducting polymers*. Boca Raton, USA: CRC Press.
- [2] Street, G. B. and Clarke, T. C., 1981. "conducting polymers: a review of recent work IBM." *J. Res. Dev.*, vol. 25, pp. 51–57.
- [3] Freund, M. S. and Deore, E. B. A., 2007. *Self doped conducting polymers*. John Wiley and Son.
- [4] Heeger, A., 2001. "Semiconducting and metallic polymers: The fourth generation of polymeric materials." *Reviews of Modern Phys.*, vol. 73, p. 681.
- [5] MacDiarmid, A. G., 2001. "A novel role for organic polymers." *Angewandte Chemie International Edition*, vol. 40, pp. 2581-2590.
- [6] Nalwa, H. S., 1977. *Ed. Handbook of organic conductive molecules and polymers*. John Wiley: Chichester, UK.

- [7] Banerjee, S. and Tayagi, A. K. E., 2012. *Functional materials, preparation, processing and applications*. Elsevier: Ailton De Souza Gomes, Ed.
- [8] Cai, Z., Grang, M., and Tang, Z., 2004. "Novel battery using conducting polymers: and polyaniline." *J. of Mater. Sci.*, vol. 39, p. 400.
- [9] Kucheldorf, H. R., Luken, O., and Swift, G., 2010. *Hand book of polymer synthesis*. 2nd ed. CRC Press.
- [10] Lange, U., Roznyatovskaya, N. V., Mirsky, and Vladimir, M., 2008. "Conducting polymers in chemical sensors and arrays." *Analytica Chimica Acta*, vol. 614, pp. 1-26.
- [11] Sapurina, I. Y. and Shishov, M. A., 2012. *New polymers for special applications*. Ailton De Souza Gomes, Ed.
- [12] Ćirić-Marjanović, G., 2010. *Polyaniline nanostructures, in nanostructured conductive polymers*, Eftekhari, A. Edit. John Wiley and Son Ltd.
- [13] Feng-Hao, Hsu, F. H., and Wu, T. M., 2012. "In situ synthesis and characterization of conductive polypyrrole/graphene composites with improved solubility and polyindole manganese oxide nanocomposite." *Indian J. of Adv conductivity*, vol. 162, pp. 682-687.
- [14] Vernitskaya, T. V., Tat'yana, V. V., and Efimov, 1977. "Polypyrrole: a conducting polymer; its synthesis, properties and applications." *Russ. Chem. Rev.*, vol. 66, p. 443.
- [15] Fajan, A. and Been, B., 2013. "Structural and optical properties of polyindole manganese oxide nanocomposite, Indian." *J. of Adv, in Chem. Sci.*, vol. 2, p. 95.
- [16] Shakshooki, S. K., Akari, F. A., Aleab, R., Ellafi, K. M., and Salima, M., 2023. *Synthesis of crystalline γ -zirconium-, mixed γ -zirconium-titanium phosphates/ polyaniline, polyindole and polycarbazole composites via oxidant cerium(IV) sulfate*. Newyork Congress, p. 992.
- [17] Shakshooki, S. K., Elakari, F. A., and Alahemmer, A. A., 2020. "Glassy-, α -zirconium-tin phosphates/ fibrous cerium(IV)Phosphate nanocomposite membranes self-supported aniline, its co-pyrrole and co-indole polymerization agent." In *The 4th International conference Theories and Application Basic and Biosciences, J.Faculty of Science University of Misurata*. pp. 335-3549.
- [18] Henrich, V. E., Henrich, V. E., and Cox, P. A., 1994. *The surface science of metal oxides*: Cambridge University Press, Cambridge Press. pp. 14-61.
- [19] Kung, H. H., 1989. *Transition metal oxides, surface chemistry and catalysis*. Amesterdam ElSevier.
- [20] West, A., 2011. *Metal oxides, basic solid state chemistry*. New York Every Science Ionic Solids.
- [21] Yang, R., Qin, J., Li, M., Yanhong, Liu, Y., and Fei, L. F., 2011. "Redox hydrothermal synthesis of cerium phosphate microspheres with different architectures." *Cryst.,Eng.Comm*, Vol 13, pp.7284-7292
- [22] Alberti, G. and Costantino, U., 1974. "Recent progress in the field of synthetic inorganic exchanger having a layered and fibrous structure." *J. Chromatogr*, vol. 102, pp. 5-29.
- [23] Casciola, M., Costantino, U., and Damico, S., 1988. "Conductivity of cerium(IV) phosphate in hydrogen form." *Solid State Ionics*, vol. 28, p. 617.
- [24] Parangi, T., Wani, P., and Chudasama, U., 2012. "Synthesis, characterization and application of cerium phosphate." *Desalination and Water Treatment*, vol. 38, p. 126.
- [25] Romano, R. and Alves, O. S., 2005. "Fibrous cerium(IV) phosphate host of weak and strong Lewis bases." *Inclus. Phenom. and Macrocyclic*, vol. 51, p. 211.
- [26] Salvado, M. A., Pertierra, P., Tropajo, C., and Garcia, G. R., 2007. "Crystal structure of cerium (iv) bis hydrogen phosphate derivative." *J. Am. Chem. Soc.*, vol. 129, p. 10970.
- [27] Conde, M., Dakhsi, K., Zouihri, H., Abdelouahdi, K., Laânab, L., Benaissa, M., and Jaber, B., 2011. "Preparation of ZrO nanoparticles without any annealing and ripening treatment." *Journal of Materials Science and Engineering*, vol. 1, pp. 985-990.
- [28] Allen, T., 1992. *Particle measurements*. 3ed ed. London: Chapman and Hall.